

Cite this: *RSC Adv.*, 2017, 7, 36895

Syntheses, crystal structures, and magnetic properties of cyclic dimer Ln_2L_2 complexes constructed from (3-pyridinylmethoxy)phenyl-substituted nitronyl nitroxide ligands†

Mei Zhu,^{ID}* Yang Li, Lingjie Jia, Li Zhang and Wei Zhang

Herein, five lanthanide-radical cyclic dimer complexes $[\text{Ln}(\text{hfac})_3(\text{NIT-3PyPh})]_2$ derived from (3-pyridinylmethoxy)phenyl-substituted nitronyl nitroxide ligands, 2-(4-(3-pyridinylmethoxy)phenyl)-4,4,5,5-tetramethyl-imidazolyl-1-oxyl-3-oxide (NIT-3PyPh), and $\text{Ln}(\text{hfac})_3$ ($\text{Ln}^{\text{III}} = \text{Gd}$ (1), Tb (2), Dy (3), Ho (4), and Er (5); hfac = hexafluoroacetylacetonato), were synthesized as well as structurally and magnetically characterized. The single-crystal structures show that these complexes are isostructural, in which the NIT-3PyPh molecule acts as a bridging ligand linking two Ln^{III} ions through the oxygen atom of the N–O group and nitrogen atom from the pyridine ring to form a four-spin system. Tb and Dy complexes exhibit a frequency-dependence of ac magnetic susceptibilities, slowing the relaxation of the magnetization.

Received 6th June 2017

Accepted 10th July 2017

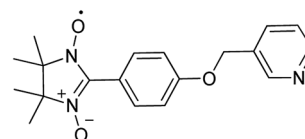
DOI: 10.1039/c7ra06310e

rsc.li/rsc-advances

Introduction

Research on single-molecule magnets (SMMs) has been a very active field and rapidly expanding for over two decades since the first magnetic dynamics of Mn_{12}Ac was discovered in the early 1990s.¹ These materials have potential applications in high-density data storage, quantum information processing systems, and spintronic devices.^{2–4} Recently, lanthanide-based systems, especially heavy lanthanide ions, have become increasingly interesting due to their large intrinsic magnetic anisotropy from the large unquenched orbital moment.⁵ This strategy has achieved tremendous success in the production of novel SMMs mainly comprising mononuclear and polynuclear pure 4f^{6,7} and mixed 3d–4f⁸ systems. However, the main disadvantage of these compounds is the internal character of their 4f unpaired electrons, which results in weak magnetic interactions between spin carriers.⁹ Nitronyl nitroxide radicals (NITs) and other organic radicals, such as verdazyl, TEMPO, TTF, and so on, as spin carriers are fascinating building blocks and bridged ligands not only for stabilization under ambient conditions but also for directed coordination to transfer effective magnetic interactions. The organic radical has proven to be an attractive route to obtain magnetically coupled 2p–4f heterospin systems.¹⁰ Contrary to 3d–4f and pure 4f metal SMMs, to date, 2p–4f SMMs are relatively rare, and only some examples

including mononuclear lanthanide–nitronyl nitroxide radical complexes,¹¹ lanthanide–nitronyl nitroxide dimers,¹² and lanthanide–biradical compounds¹³ have been reported. As is known, discrete complexes with definite geometry resulting from paramagnetic metal ions and organic radicals are good candidates for the fundamental studies of magneto-structural correlations, in particular for determining how the structural factors affect the interaction between metals and nitronyl nitroxide and how to improve magnetic relaxation.¹⁴ Moreover, for nitronyl nitroxide–Ln complexes, several investigations have shown that the substituents of the nitronyl nitroxide radicals play a crucial role in modulating the dynamics of magnetization.¹⁵ Herein, a (3-pyridinylmethoxy)phenyl-substituted nitronyl nitroxide radical, NIT-3PyPh (NIT-3PyPh = 2-(4-(3-pyridinylmethoxy)phenyl)-4,4,5,5-tetramethyl-imidazolyl-1-oxyl-3-oxide, Scheme 1), is chosen to assemble a series of 2p–4f compounds. This radical ligand not only has a functional coordinated atom but also shows a long and flexible substituted group relativity as compared to the pyridine or benzene-substituted radical, which may construct the variety structures of complexes. In this study, the complexes are isostructural, exhibiting cyclic nitronyl nitroxide–Ln dimer units in which two NIT-3PyPh radicals act as



Scheme 1 NIT-3PyPh ligand.

Department of Chemistry, Zhejiang Sci-Tech University, Hangzhou 310018, China.
E-mail: zhumei0321@163.com

† Electronic supplementary information (ESI) available. CCDC 1538537–1538541. For ESI and crystallographic data in CIF or other electronic format see DOI: 10.1039/c7ra06310e



bridging ligands to link two Ln(hfac)₃ units through the oxygen atoms of the nitroxide groups and nitrogen atoms of the pyridine ring, namely [Ln(hfac)₃(NIT-3PyPh)]₂(Ln^{III} = Gd (1), Tb (2), Dy (3), Ho (4), and Er (5)); hfac = hexafluoroacetylacetonato). Magnetic studies show that Tb and Dy complexes exhibit slow magnetic relaxation, the typical characteristic of SMMs.

Experimental

Materials and physical measurements

All the reagents and chemicals used in the syntheses were of analytical grade. Ln(hfac)₃·2H₂O and the radical ligand NIT-3PyPh were prepared according to the literature methods.¹⁶ Elemental analyses for carbon, hydrogen, and nitrogen were carried out using a Perkin-Elmer 240 elemental analyzer. Infrared spectra were obtained from KBr pellets in the 4000–400 cm⁻¹ region *via* a Bruker Tensor 27FTIR spectrophotometer. Magnetic measurements were conducted using a Quantum Design VSM SQUID magnetometer. Diamagnetic corrections were made with Pascal's constants for all of the constituent atoms and sample holders.

Synthesis

Compounds 1–5 [Ln(hfac)₃(NIT-3PyPh)]₂(Ln^{III} = Gd (1), Tb (2), Dy (3), Ho (4), and Er (5)) were obtained *via* the same procedure. A suspension of 0.02 mmol Ln(hfac)₃·2H₂O in 20 mL *n*-heptane was heated to reflux for about 2 hours. Then, the solution was subsequently cooled to 90 °C; after this, 0.02 mmol NIT-3PyPh in 10 mL dichloromethane was added under stirring. The mixture was refluxed for another 1 hour and then cooled to room temperature. The filtrate was allowed to stay at room temperature for slow evaporation. After two days, dark-blue block crystals suitable for single-crystal X-ray analysis were obtained.

[Gd(hfac)₃(NIT-3PyPh)]₂ (1). Yield: 76%. Anal. calc. for C₆₈H₅₀F₃₆Gd₂N₆O₁₈: C, 36.50, H, 2.25, N, 3.76; found: C, 36.66, H, 2.42, N, 3.93%. IR (KBr, cm⁻¹): 3432 (m), 1654 (s), 1510 (m), 1260 (s), 1208 (s), 1147 (s), 799 (m), 662 (m).

[Tb(hfac)₃(NIT-3PyPh)]₂ (2). Yield: 72%. Anal. calc. for C₆₈H₅₀F₃₆Tb₂N₆O₁₈: C, 36.45, H, 2.25, N, 3.75; found: C, 36.51, H, 2.32, N, 4.14%. IR (KBr, cm⁻¹): 3433 (m), 1655 (s), 1512 (m), 1259 (s), 1205 (s), 1146 (s), 798 (m), 661 (m).

[Dy(hfac)₃(NIT-3PyPh)]₂ (3). Yield: 74%. Anal. calc. for C₆₈H₅₀F₃₆Dy₂N₆O₁₈: C, 36.33, H, 2.24, N, 3.74; found: C, 36.21, H, 2.12, N, 3.95%. IR (KBr, cm⁻¹): 3433 (m), 1658 (s), 1505 (m), 1259 (s), 1208 (s), 1148 (s), 800 (m), 661 (m).

[Ho(hfac)₃(NIT-3PyPh)]₂ (4). Yield: 71%. Anal. calc. for C₆₈H₅₀F₃₆Dy₂N₆O₁₈: C, 36.25, H, 2.24, N, 3.73; found: C, 36.31, H, 2.29, N, 3.67%. IR (KBr, cm⁻¹): 3432 (m), 1658 (s), 1505 (m), 1259 (s), 1208 (s), 1148 (s), 800 (m), 661 (m).

[Er(hfac)₃(NIT-3PyPh)]₂ (5). Yield: 79%. Anal. calc. for C₆₈H₅₀F₃₆Er₂N₆O₁₈: C, 36.18, H, 2.23, N, 3.72; found: C, 36.29, H, 2.45, N, 3.93%. IR (KBr, cm⁻¹): 3432 (m), 1655 (s), 1512 (m), 1259 (s), 1205 (s), 1146 (s), 798 (m), 661 (m).

X-ray data collection and structure refinement

All crystallographic data were obtained using a Rigaku CCD diffractometer with graphite monochromated Mo K α radiation ($\lambda = 0.71073$ Å) at 113 K. Structures were solved *via* direct methods using the SHELXS-2014 program and refined by a full-matrix least-squares techniques against F^2 with the SHELXTL-2014 program package.¹⁷ Some restraints are applied, such as ISOR, DFIX, to solve the disorder of the F atoms. Besides fluorine atoms, all other non-hydrogen atoms were anisotropically refined, and hydrogen atoms were fixed at the calculated positions, which were refined using a riding model. The pertinent crystallographic data and structure refinement parameters for complexes 1–5 are listed in Table 1. The important bond lengths

Table 1 Crystal data and structure refinement for complexes 1–5

	1 Gd	2 Tb	3 Dy	4 Ho	5 Er
Formula	C ₆₈ H ₅₀ F ₃₆ Ln ₂ N ₆ O ₁₈				
M_r	2237.63	2241.98	2248.12	2252.99	2257.64
T , K	113(2)	293(2)	113(2)	113(2)	113(2)
λ (Mo K α), Å	0.71073				
Crystal system	Monoclinic	Monoclinic	Monoclinic	Monoclinic	Monoclinic
Space group	$P2_1/n$	$P2_1/c$	$P2_1/c$	$P2_1/c$	$P2_1/c$
a , Å	13.433(3)	13.504(3)	13.394(3)	13.372(3)	13.387(3)
b , Å	17.289(4)	17.675(3)	17.257(3)	17.214(3)	17.241(3)
c , Å	18.334(4)	22.376(7)	22.104(7)	22.022(7)	22.063(7)
α , deg	90				
β , deg	93.07(3)	124.48(2)	124.21(2)	124.08(2)	124.00(2)
γ , deg	90				
V , Å ³	4252.0(15)	4402.5(18)	4225.2(18)	4198.5(18)	4221.7(18)
Z	2				
D_c , g cm ⁻³	1.748	1.690	1.767	1.782	1.776
μ , mm ⁻¹	1.692	1.734	1.902	2.018	2.121
θ range, deg	1.62–25.01	1.60–25.01	1.62–25.01	1.63–27.97	1.62–25.01
Unique reflns/ R_{int}	7492/0.0463	7726/0.0409	7439/0.0491	10 025/0.0546	7426/0.0445
GOF	1.05	1.069	1.038	1.023	1.070
R_1 [$I > 2\sigma(I)$]	0.0603	0.0719	0.0577	0.0642	0.0571
wR_2 [$I > 2\sigma(I)$]	0.1687	0.1925	0.1648	0.1791	0.1663



Table 2 The important bond distances (Å) and angles (°) for complexes 1–5

Complexes	Bond lengths Ln–O(rad)	Bond lengths Ln–N(py)	Angle of O(rad)–Ln–N(py)	Dihedral angle between the phenyl plane and the nitroxide plane	Dihedral angle between the phenyl plane and the pyridine plane
1	2.320(5)	2.579(5)	71.91(17)	36.46	48.74
2	2.317(6)	2.585(6)	72.0(2)	37.10	48.96
3	2.294(5)	2.560(5)	71.74(17)	36.39	48.96
4	2.282(4)	2.547(5)	71.74(16)	35.97	49.01
5	2.281(5)	2.534(6)	71.75(18)	36.07	49.02

and angles for 1–5 are listed in Tables 2 and S1–S5.† CCDC 1538537–1538541.†

Results and discussion

Crystal structure

Single-crystal X-ray diffraction analyses reveal that complexes 1–5 are isomorphous; therefore, only the structure of complex 1 has been described in detail. Complex 1 crystallizes in the monoclinic space group $P2_1/n$ with the central symmetric structure. Moreover, two NIT-3PyPh paramagnetic ligands are linked through coordination bonds with two molecules of $Gd(hfac)_3$ to generate a four-spin cyclic dimer complex (Fig. 1). Gd^{III} is coordinated with six oxygen atoms from three hfac ligands and one oxygen atom and one nitrogen atom from two different nitronyl nitroxide units to form a distorted square antiprism geometry. As is known, eight coordinate geometries refer to some polyhedra, including D_{2d} dodecahedron (DD), D_{4d} square antiprism (SAPR), C_{2v} bicapped trigonal prism (TPRS), and so on. Continuous shape measures have been performed with SHAPE to evaluate the actual shape of the coordination spheres of the Ln atoms for complexes 1–5¹⁸(Table 3), indicating that all of them are located in distorted square antiprism environments. The NIT-3PyPh molecule acts as a bidentate bridging ligand to link two Gd^{III} ions by the oxygen atom of the nitroxide group and the nitrogen atom of the pyridine ring. Within a dimer unit, the phenyl ring of one NIT-3PyPh ligand is almost parallel to the pyridine group of the other NIT-3PyPh molecule; this may due to the π – π stacking interaction between the phenyl ring and the pyridine ring. The bond lengths of Gd^{III} –O (nitroxide) and Gd^{III} –N are 2.320(5) and 2.579(5) Å, respectively, which are comparable to those reported for other lanthanide–pyridine-substituted radical complexes.^{12a,b} In the dimer units, the distance of two metal ions is 11.675 Å. The shortest intermolecular Gd^{III} – Gd^{III} distance is 9.272 Å, whereas the nearest contact between the uncoordinated N–O groups is 3.546 Å (Fig. 2), which implies that there is non-negligible magnetic coupling between uncoordinated NO groups. The crystal structures and packing arrangements for the complexes 2–5 are shown in Fig. S1–S4 and S5–S8,† respectively.

Magnetic properties

The temperature-dependent magnetic susceptibility data of complexes 1–5 were measured in the range of 2–300 K under

an external magnetic field of 1 kOe (Fig. 3). At room temperature, the $\chi_M T$ values are 16.84, 24.99, 29.02, 29.68, and 25.04 $cm^3 K mol^{-1}$ for compounds 1, 2, 3, 4, and 5, respectively, which are close to the expected values of 16.51, 24.39, 29.09,

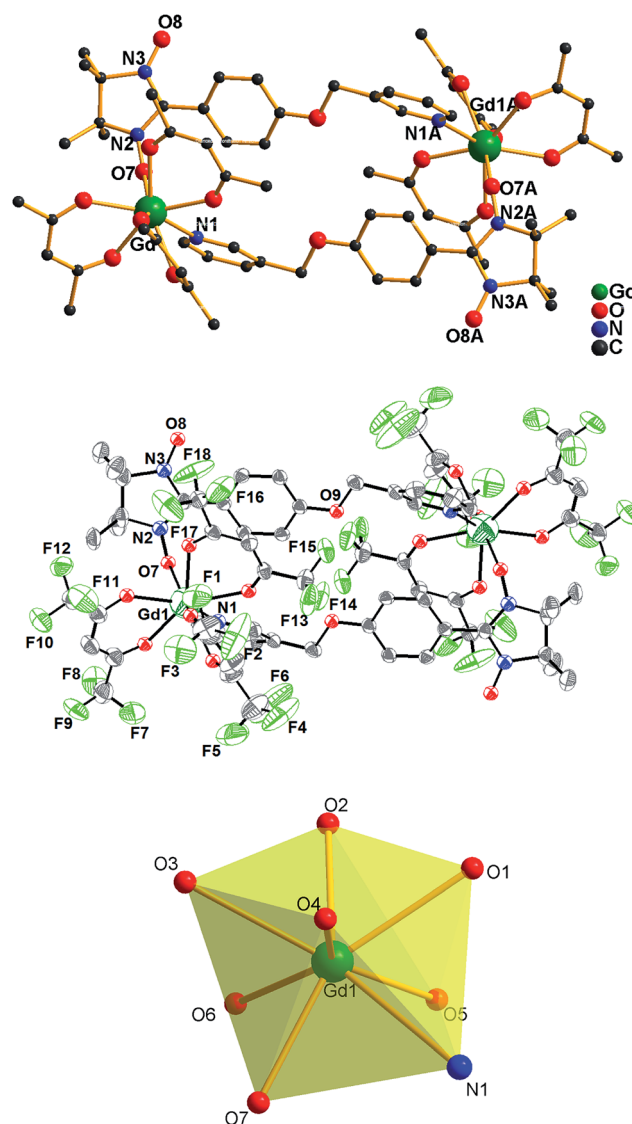


Fig. 1 (Top) Crystal structure of complex 1, (H atoms and F atoms are omitted for clarity and symmetry transformations used to generate equivalent atoms A: $2 - x, 2 - y, -z$); (middle) ORTEP view of complex 1 at the 50% probability level. (Bottom) The coordination polyhedron of $Gd^{(III)}$ ion in 1.



Table 3 Lanthanide geometry analysis using the Shape software for complexes 1–5

Complex	Ln	D_{4d} SAPR	D_{2d} DD	C_{2v} TPRS
1	Gd	0.789	1.877	1.833
2	Tb	0.792	2.025	1.798
3	Dy	0.777	1.901	1.808
4	Ho	0.750	1.908	1.782
5	Er	0.739	1.907	1.764

28.89, and 23.71 $\text{cm}^3 \text{K mol}^{-1}$ for the uncoupled two Ln^{III} ions (Gd^{III} : $^8\text{S}_{7/2}$, $S = 7/2$, $L = 0$, $J = 7/2$, $g = 2$, $C = 7.88 \text{ cm}^3 \text{K mol}^{-1}$; Tb^{III} : $^7\text{F}_6$, $S = 3$, $L = 3$, $J = 6$, $g = 3/2$, $C = 11.82 \text{ cm}^3 \text{K mol}^{-1}$; Dy^{III} : $^6\text{H}_{15/2}$, $S = 5/2$, $L = 5$, $J = 15/2$, $g = 4/3$, $C = 14.17 \text{ cm}^3 \text{K mol}^{-1}$; Ho^{III} : $^5\text{I}_8$, $S = 2$, $L = 6$, $J = 8$, $g = 5/4$, $C = 14.08 \text{ cm}^3 \text{K mol}^{-1}$; and Er^{III} : $^4\text{H}_{15/2}$, $S = 3/2$, $L = 6$, $J = 15/2$, $g = 6/5$, $C = 11.48 \text{ cm}^3 \text{K mol}^{-1}$) plus two organic radicals NIT-3PyPh ($S = 1/2$). For the complex of **1**, upon cooling, the $\chi_{\text{M}}T$ value remains almost constant until 74 K and then decreases more and more dramatically to reach a value of 13.62 $\text{cm}^3 \text{K mol}^{-1}$ at 2 K. As is known, there are mainly three kinds of magnetic interactions based on the present magnetic system: (i) Gd^{III} ion interacting with the directly coordinated NO group (J_1); (ii) the magnetic coupling between two uncoordinated NO groups through space (J_2); and (iii) Gd^{III} ion interacting with the NO group through the pyridine and benzene ring. However, the last interaction should be weak¹⁹ and could be neglected. Hence, the magnetic behavior of **1** can be interpreted as that of one linear Gd–rad–rad–Gd magnetic unit (Scheme 2). According to the structural data, the torsion angle for Gd–O–N–C is 77.5°, and the value of J_1 should be positive.²⁰ Therefore, the observed antiferromagnetic coupling in complex **1** may be due to the strong magnetic coupling between two uncoordinated NO groups, which overwhelm the ferromagnetic interaction between Gd and the directed coordinated NO group.²¹ MAGPACK²² software was used to simulate the magnetic susceptibilities based on the Hamiltonian equation: $\hat{H} =$

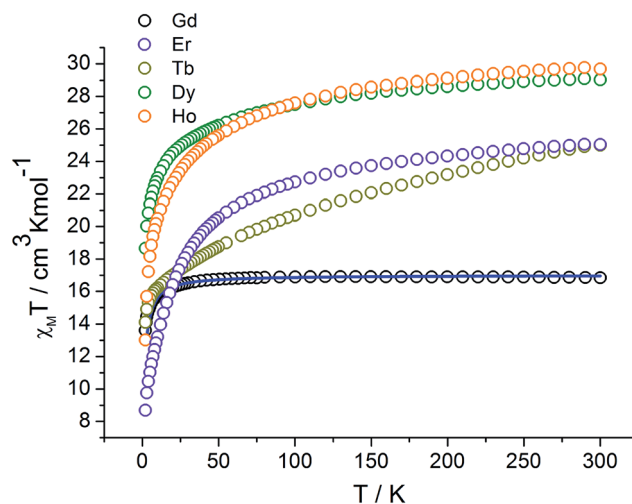
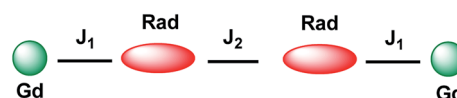


Fig. 3 $\chi_{\text{M}}T$ versus T plots of complexes 1–5; the solid line represents the best-fitted simulation curve using MAGPACK.



Scheme 2 The magnetic exchange pathways in complex **1**.

$-2J_1(\hat{S}_{\text{Rad}1}\hat{S}_{\text{Gd}1} + \hat{S}_{\text{Rad}2}\hat{S}_{\text{Gd}2}) - 2J_2\hat{S}_{\text{Rad}1}\hat{S}_{\text{Rad}2}$ and the best agreement between calculated and experimental behaviors was obtained for $J_1 = 1.89 \text{ cm}^{-1}$, $J_2 = -18.39 \text{ cm}^{-1}$, and $g = 2.01$. The positive J_1 is in agreement with a weak ferromagnetic interaction between Gd(III) and the NO group, as was already observed in other gadolinium nitronyl nitroxide compounds.²³ The large negative J_2 indicates that there exists important antiferromagnetic interaction between uncoordinated NO groups. For complexes **2**, **3**, **4**, and **5**, the $\chi_{\text{M}}T$ values continuously decrease with the decreasing temperature and reach minimum values of 14.10, 18.66, 13.02, and 8.69 $\text{cm}^3 \text{K mol}^{-1}$ at 2 K, respectively. The

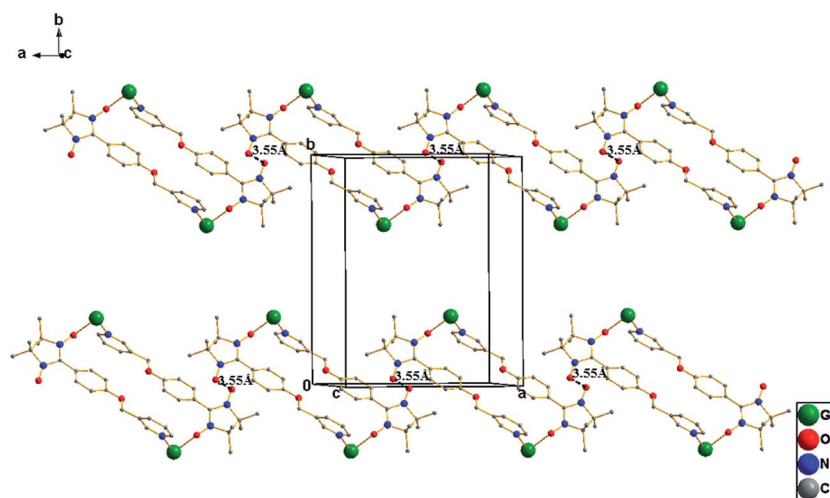


Fig. 2 Packing diagram of complex **1**, hfac ligands and hydrogen and fluorine atoms are not shown for clarity.



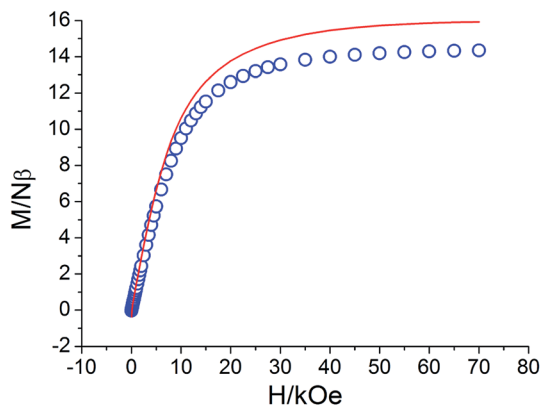


Fig. 4 M versus H plot at 2 K for complex 1. The solid line represents the Brillouin function for non-coupled two $S = 7/2$ and two $S = 1/2$ spin centers ($g = 2.0$, $T = 2$ K).

overall behaviors of compounds 2–5 can be ascribed to the depopulation of Ln(III) ion Stark sublevels and magnetic couple interaction within the complexes.

The field-dependent magnetizations of 1–5 at 2.0 K are shown in Fig. 4 and S9.† For complex 1, upon increasing the applied field, M increases up to 14.34 $N\beta$ at 70 kOe. For any value of the field, the experimental magnetization value is lower than the magnetization calculated by the Brillouin function for non-coupled two $S = 7/2$ and two $S = 1/2$ spins ($g = 2.0$ and $T = 2$ K), further supporting the antiferromagnetic interactions in this compound. For complexes 2, 3, 4, and 5, the magnetization reveals a rapid increase at low field and reaches 8.53, 12.03, 11.99, and 10.43 $N\beta$ at 70 kOe, respectively. All the M values did not reach the expected saturation values; this suggested the presence of magnetic anisotropy and/or low-lying excited states in the systems.

AC magnetic susceptibility measurements were carried out for 2 and 3 to probe dynamic magnetic behaviors. For compound 2, as shown in Fig. 5, in a zero dc field with an ac field of 2 Oe, both the in-phase (χ') and out-of-phase (χ'') components of ac susceptibility showed frequency dependence; this suggested the presence of slow magnetic relaxation at low temperatures. According to the magnetic couplings, the quantum tunneling of the magnetization (QTM) is reduced

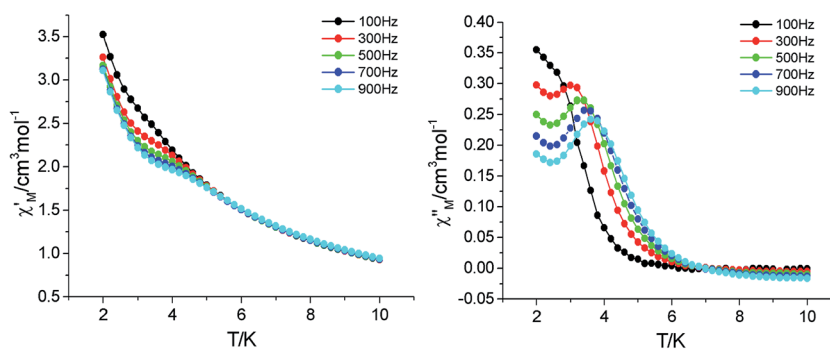


Fig. 5 Temperature dependence of the in-phase (left) and out-of-phase (right) plots for 2 at frequencies 100–900 Hz with $H_{dc} = 0$ and $H_{ac} = 2$ Oe.

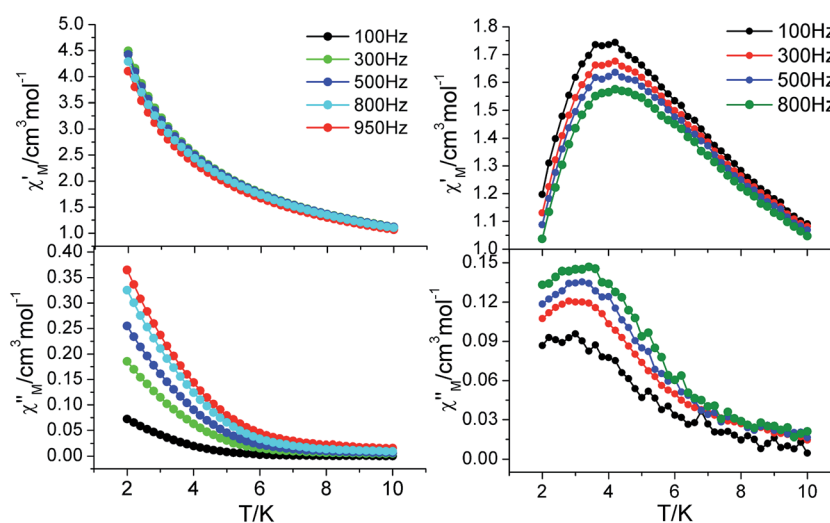


Fig. 6 Temperature dependence of the in-phase and out-of-phase components of the ac magnetic susceptibility for 3 in zero (left) and 5 kOe (right) dc fields with an oscillation of 2 Oe.



when the unit is exchange coupled with neighboring magnetic centers, which allows the observation of the magnetic relaxation behavior even without an applied field. The peaks of the out-of-phase signals are visible and follow the Arrhenius law $\tau = \tau_0 \exp(\Delta/k_B T)$ with the pre exponential factor $\tau_0 = 4.04 \times 10^{-7}$ s and the effective anisotropy barrier $\Delta/k_B = 21.6$ K. Compared with those of the reported cyclic Tb-radical complexes,¹² the value of this barrier is almost high, especially in the zero dc field. (Fig. S10†).

Complex 3 shows frequency-dependent out-of-phase signals in a zero dc field with an ac field of 2 Oe (Fig. 6); however, there is no maxima visible down to 2.0 K. This behavior may result from the relaxation mechanism such as quantum tunneling of the magnetization (QTM). Since the tunneling mechanism might be suppressed *via* application of a static magnetic field,²⁴ we obtained ac susceptibility *vs.* temperature in 5 kOe dc field. As expected, both in-phase (χ') and out-of-phase (χ'') signals are more visible and show frequency dependent peaks, indicating similar SMMs behavior. Fitting the data to the Arrhenius law (Fig. S11†) gives the pre-exponential factor $\tau_0 = 3.31 \times 10^{-9}$ s and the effective anisotropy barrier $\Delta/k_B = 35.47$ K.

Conclusion

In conclusion, five new cyclic lanthanide-radical compounds [Ln(hfac)₃(NIT-3PyPh)]₂ have been synthesized. The investigation of the dynamics of the magnetization for complexes 2 and 3 shows that they exhibit SMMs behavior; especially, the peaks of the out-of-phase signals are visible in a zero dc field for the Tb compound. Contrary to the other Ln-based SMMs, reports on Tb-based SMMs are rare because the bistability is not guaranteed for non-Kramer Tb(III) ions. The results demonstrated that the substituents of the radicals play a crucial role in the magnetic behaviors, and minor structural changes can induce large differences for magnetic relaxation. This strategy is promising to design new lanthanide-radical SMM molecular magnetic materials.

Acknowledgements

This work was supported by the National Natural Science Foundation of China (No. 21602202), the Natural Science Foundation of Zhejiang Province (No. LQ17B010005), and the Science Foundation of Zhejiang Sci-Tech University (No. 15062094-Y). We thank Professor Licun Li of Nankai University for guidance.

References

- (a) R. Sessoli, D. Gatteschi, A. Caneschi and M. A. Novak, *Nature*, 1993, **365**, 141; (b) R. Sessoli, H. L. Tsai, A. R. Schake, S. Wang, J. B. Vincent, K. Folting, D. Gatteschi, G. Christou and D. N. Hendrickson, *J. Am. Chem. Soc.*, 1993, **115**, 1804.
- M. Mannini, F. Pineider, P. Saintavitt, C. Danieli, E. Otero, C. Sciancalepore, A. M. Talarico, M. A. Arrio, A. Cornia, D. Gatteschi and R. Sessoli, *Nat. Mater.*, 2009, **8**, 194.
- (a) M. N. Leuenberger and D. Loss, *Nature*, 2001, **410**, 789; (b) A. Ardavan, O. Rival, J. J. L. Morton, S. J. Blundell, A. M. Tyryshkin, G. A. Timco and R. E. P. Winpenny, *Phys. Rev. Lett.*, 2007, **98**, 057201.
- (a) L. Bogani and W. Wernsdorfer, *Nat. Mater.*, 2008, **7**, 179; (b) M. J. Graham, J. M. Zadrozny, M. Shiddiq, J. S. Anderson, M. S. Fataftah, S. Hill and D. E. Freedman, *J. Am. Chem. Soc.*, 2014, **136**, 7623.
- (a) R. Sessoli and A. K. Powell, *Coord. Chem. Rev.*, 2009, **253**, 2328; (b) D. N. Woodruff, R. E. P. Winpenny and R. A. Layfield, *Chem. Rev.*, 2013, **113**, 5110.
- (a) N. Ishikawa, M. Sugita, T. Ishikawa, S. Koshihara and Y. Kaizu, *J. Am. Chem. Soc.*, 2003, **125**, 8694; (b) S. D. Jiang, B. W. Wang, H. L. Sun and S. Gao, *J. Am. Chem. Soc.*, 2011, **133**, 4730; (c) S. Cardona-Serra, J. M. Clemente-Juan, E. Coronado, A. Gaita-Ariño, A. Camón, M. Evangelisti, F. Luis, M. J. Martíñez-Pérez and J. Sesé, *J. Am. Chem. Soc.*, 2012, **134**, 14982; (d) J. Liu, Y. C. Chen, J. L. Liu, V. Vieru, L. Ungur, J. H. Jia, L. F. Chibotaru, Y. Lan, W. Wernsdorfer, S. Gao, X. M. Chen and M. L. Tong, *J. Am. Chem. Soc.*, 2016, **138**, 5441.
- (a) R. J. Blagg, C. A. Muryn, E. J. L. McInnes, F. Tuna and R. E. P. Winpenny, *Angew. Chem., Int. Ed.*, 2011, **50**, 6530; (b) Y. F. Bi, X. T. Wang, W. P. Liao, X. W. Wang, R. P. Deng, H. J. Zhang and S. Gao, *Inorg. Chem.*, 2009, **48**, 11743; (c) X. J. Zhang, V. Vieru, X. W. Feng, J. L. Liu, Z. J. Zhang, B. Na, W. Shi, B. W. Wang, A. K. Powell, L. F. Chibotaru, S. Gao, P. Cheng and R. Jeffrey, *Angew. Chem., Int. Ed.*, 2015, **54**, 9861; (d) R. J. Blagg, L. Ungur, F. Tuna, J. Speak, P. Comar, D. Collison, W. Wernsdorfer, E. J. L. McInnes, L. F. Chibotaru and R. E. P. Winpenny, *Nat. Chem.*, 2013, **5**, 673.
- (a) G. Novitchi, W. Wernsdorfer, L. F. Chibotaru, J. P. Costes, C. E. Anson and A. K. Powell, *Angew. Chem., Int. Ed.*, 2009, **48**, 1614; (b) T. C. Stamatas, S. J. Teat, W. Wernsdorfer and G. Christou, *Angew. Chem., Int. Ed.*, 2009, **48**, 521; (c) V. M. Mereacre, A. M. Ako, R. Clérac, W. Wernsdorfer, G. Filoti, J. Bartolomé, C. E. Anson and A. K. Powell, *J. Am. Chem. Soc.*, 2007, **129**, 9248; (d) M. Andruh, J.-P. Costes, C. Diaz and S. Gao, *Inorg. Chem.*, 2009, **48**, 3342; (e) J. L. Liu, J. Y. Wu, Y. C. Chen, V. Mereacre, A. K. Powell, L. Ungur, L. F. Chibotaru, X. M. Chen and M. L. Tong, *Angew. Chem., Int. Ed.*, 2014, **53**, 12966; (f) T. Pugh, N. F. Chilton and R. A. Layfield, *Angew. Chem., Int. Ed.*, 2016, **55**, 11082.
- (a) M. Andruh, I. Ramade, E. Codjovi, O. Guillou, O. Kahn and J. C. Trombe, *J. Am. Chem. Soc.*, 1993, **115**, 1822; (b) J.-P. Costes, F. Dahan, A. Dupuis and J.-P. Laurent, *Chem.–Eur. J.*, 1998, **4**, 1616; (c) F. Habib and M. Murugesu, *Chem. Soc. Rev.*, 2013, **42**, 3278.
- (a) J. D. Rinehart, M. Fang, W. J. Evans and J. R. Long, *J. Am. Chem. Soc.*, 2011, **133**, 14236; (b) G. Poneti, K. Bernot, L. Bogani, A. Caneschi, R. Sessoli, W. Wernsdorfer and D. Gatteschi, *Chem. Commun.*, 2007, 1807; (c) K. Bernot, L. Bogani, A. Caneschi, D. Gatteschi and R. Sessoli, *J. Am. Chem. Soc.*, 2006, **128**, 7947; (d) F. Pointillart, B. L. Guennic, S. Golhen, O. Cador and L. Ouahab, *Chem.*



- Commun.*, 2013, **49**, 11632; (e) E. M. Fatila, M. Rouzières, M. C. Jennings, A. J. Lough, R. Clérac and K. E. Preuss, *J. Am. Chem. Soc.*, 2013, **135**, 9596; (f) S. Demir, J. M. Zadrozny, M. Nippe and J. R. Long, *J. Am. Chem. Soc.*, 2012, **134**, 18546; (g) S. G. Reis, M. Briganti, S. Soriano, G. P. Guedes, S. Calancea, C. Tiseanu, M. A. Novak, M. A. del Águila-Sánchez, F. Totti, F. Lopez-Ortiz, M. Andruh and M. G. F. Vaz, *Inorg. Chem.*, 2016, **55**, 11676; (h) F. Pointillart, J. Jung, R. Berraud-Pache, B. L. Guennic, V. Dorcet, S. Golhen, O. Cador, O. Maury, Y. Guyot, S. Decurtins, S.-X. Liu and L. Ouahab, *Inorg. Chem.*, 2015, **54**, 5384.
- 11 (a) N. Zhou, Y. Ma, C. Wang, G. F. Xu, J. K. Tang, J. X. Xu, S. P. Yan, P. Cheng, L. C. Li and D. Z. Liao, *Dalton Trans.*, 2009, 8489; (b) A. Lannes, M. Intissar, Y. Suffren, C. Reber and D. Luneau, *Inorg. Chem.*, 2014, **53**, 9548; (c) X. L. Wang, L. C. Li and D. Z. Liao, *Inorg. Chem.*, 2010, **49**, 4735; (d) A. Lannes, M. Intissar, Y. Suffren, C. Reber and D. Luneau, *Inorg. Chem.*, 2014, **53**, 9548.
- 12 (a) J. X. Xu, Y. Ma, D. Z. Liao, G. F. Xu, J. K. Tang, C. Wang, N. Zhou, S. P. Yan, P. Cheng and L. C. Li, *Inorg. Chem.*, 2009, **48**, 8890; (b) X. L. Mei, R. N. Liu, C. Wang, P. P. Yang, L. C. Li and D. Z. Liao, *Dalton Trans.*, 2012, 2904; (c) F. Pointillart, K. Bernot, G. Poneti and R. Sessoli, *Inorg. Chem.*, 2012, **51**, 12218; (d) R. N. Liu, C. M. Zhang, L. C. Li, D. Z. Liao and J.-P. Sutter, *Dalton Trans.*, 2012, 12139; (e) H. X. Tian, R. N. Liu, X. L. Wang, P. P. Yang, Z. X. Li, L. C. Li and D. Z. Liao, *Eur. J. Inorg. Chem.*, 2009, 4498.
- 13 (a) K. Bernot, F. Pointillart, P. Rosa, M. Etienne, R. Sessoli and D. Gatteschi, *Chem. Commun.*, 2010, **46**, 6458; (b) S. G. Reis, M. Briganti, D. O. T. A. Martins, H. Akpınar, S. Calancea, G. P. Guedes, S. Soriano, M. Andruh, R. A. A. Cassaro, P. M. Lahti, F. Totti and M. G. F. Vaz, *Dalton Trans.*, 2016, 2936; (c) X. Li, T. Li, L. Tian, Z. Y. Liu and X. G. Wang, *RSC Adv.*, 2015, **5**, 74864.
- 14 (a) K. E. Vostrikova, D. Luneau, W. Wernsdorfer, P. Rey and M. Verdaguer, *J. Am. Chem. Soc.*, 2000, **122**, 718; (b) F. L. de Panthou, E. Belorizky, R. Calemczuk, D. Luneau, C. Marcenat, E. Ressouche, P. Turek and P. Rey, *J. Am. Chem. Soc.*, 1995, **117**, 11247.
- 15 (a) L. Bogani, C. Sangregorio, R. Sessoli and D. Gatteschi, *Angew. Chem., Int. Ed.*, 2005, **44**, 5817; (b) R. N. Liu, Y. Ma, P. P. Yang, X. Y. Song, G. F. Xu, J. K. Tang, L. C. Li, D. Z. Liao and S. P. Yan, *Dalton Trans.*, 2010, 3321.
- 16 M. Zhu, M. Yang, J. J. Wang, H. D. Li and L. C. Li, *Chem.-Asian J.*, 2016, **11**, 1900.
- 17 (a) G. M. Sheldrick, *SHELXL-2014, Program for Structures Solution*, University of Göttingen, Germany, 1997; (b) G. M. Sheldrick, *SHELXS-2014, Program for Structures Refinement*, University of Göttingen, Germany, 1997.
- 18 (a) D. Casanova, M. Llunell, P. Alemany and S. Alvarez, *Chem.-Eur. J.*, 2005, **11**, 1479; (b) M. Llunell, D. Casanova, J. Cirera, P. Alemany and S. Alvarez, *SHAPE, version 2.1*, University of Barcelona, Barcelona, 2013.
- 19 C. Benelli, A. Caneschi, D. Gatteschi and L. Pardi, *Inorg. Chem.*, 1992, **31**, 741.
- 20 T. Kanetomo and T. Ishida, *Inorg. Chem.*, 2014, **53**, 10794.
- 21 (a) C. Benelli, A. Caneschi, D. Gatteschi, L. Pardi, P. Rey, D. P. Shum and R. L. Carlin, *Inorg. Chem.*, 1989, **28**, 272; (b) R. N. Liu, L. C. Li, X. L. Wang, P. P. Yang, C. Wang, D. Z. Liao and J.-P. Sutter, *Chem. Commun.*, 2010, **46**, 2566; (c) J.-P. Sutter, M. L. Kahn, S. Golhen, L. Ouahab and O. Kahn, *Chem.-Eur. J.*, 1998, **4**, 571; (d) M. Yang, H. D. Li and L. C. Li, *Inorg. Chem. Commun.*, 2017, **76**, 59.
- 22 (a) J. J. Borrás-Almenar, J. M. Clemente-Juan, E. Coronado and B. S. Tsukerblat, *Comput. Chem.*, 2001, **22**, 985; (b) J. J. Borrás-Almenar, J. M. Clemente-Juan, E. Coronado and B. S. Tsukerblat, *Inorg. Chem.*, 1999, **38**, 6081.
- 23 (a) C. Benelli, A. Caneschi, D. Gatteschi, J. Laugier and P. Rey, *Angew. Chem., Int. Ed.*, 1987, **26**, 913; (b) C. Lescop, D. Luneau, P. Rey, G. Bussière and C. Reber, *Inorg. Chem.*, 2002, **41**, 5566.
- 24 L. Thomas, F. Lioni, R. Ballou, D. Gatteschi, R. Sessoli and B. Barbara, *Nature*, 1996, **383**, 145.

